ELSEVIER

European Journal of Pharmaceutics and Biopharmaceutics 46 (1998) 169–175

European Journal of Pharmaceutics and Biopharmaceutics

Research paper

Dependence between dissolution rate and porosity of compressed erythromycin acistrate tablets

Merja Riippi[a,*], Jouko Yliruusi[a], Tapani Niskanen[b], Juha Kiesvaara[b]

[a]*Pharmaceutical Technology Division, University of Helsinki, Helsinki, Finland*
[b]*Orion Corporation, Orion Pharma, R & D, Espoo, Finland*

Received 15 May 1997; revised version received 10 December 1997; accepted 10 December 1997

Abstract

The correlation between dissolution rate and porosity of compressed erythromycin acistrate tablets was studied. The total porosity of the tablets, the pore size distribution and the specific surface area of the pores were determined using high-pressure mercury porosimetry. The particle size and specific surface area of the raw material and of the dry granulated mass of the tablets were also determined. The results show that the pore size distribution, showing the differences in pore structure, is more informative than total intruded volume of mercury. However, it is very difficult to explain the dissolution behaviour of erythromycin acistrate tablets only by porosity results of the tablets, and more work is still needed in this field.

Keywords: High-pressure mercury porosimetry; Porosity; Pore size distribution; Dissolution rate; Tablet; Erythromycin acistrate

1. Introduction

High-pressure mercury porosimetry is one of the best methods to study the microstructure of tablets. The principle of the method is based on a non-wetting behaviour of mercury towards most substances. This is why mercury does not penetrate freely into the pores and openings of the compressed tablets, and thus external pressure must be applied to achieve penetration. The theory of mercury porosimetry is based on Washburn's equation [1], which binds together the pressure and the radius of the pores:

$$P \times r = -2 \times \gamma \times \cos\theta \quad (1)$$

where P is pressure, r is radius, γ is surface tension (480 mN/m) and θ is contact angle (140°) of mercury against the studied material [2,3]. The use of Washburn's equation is based on a few basic assumptions: the shape of the neck of the pore is assumed to be circular, and the surface tension of mercury and the contact angle are considered to be constant.

In 1945, the first equipment for measuring mercury intrusion was introduced by Ritter and Drake [4] and in 1956 Strickland et al. reported the first application of mercury porosimetry for determining the porosity of pharmaceutical granules [5]. The pressure range used was 16–187 kPa (pore diameter 8–92 μm). Recently, application of mercury porosimetry in pharmaceutical technology was reviewed by Dees and Polderman [6].

The penetration of liquid into porous matrix is strongly affected by mean pore size and pore size distribution [7]. If the majority of the pores are large, penetration is more rapid than if the majority of the pores are small. Selkirk and Ganderton stated that the narrower pore size distribution contributes to slower penetration by water but to greater saturation of the tablets with the liquid [8]. Juppo has studied the porosity of lactose, glucose and mannitol granules and also porosity of the corresponding tablets. She concluded that the behaviour of granule pore structure is highly

* Corresponding author. Pharmaceutical Technology Division, University of Helsinki, P.O. Box 56, Helsinki, Finland 00014. Tel.: +358 708 59144.

0939-6411/98/$19.00
PII S0939-6411(98)00003-4

dependent on the solubility, and on the intrinsic dissolution rate and native particle size of the granule material. The advantages of pore volume size distribution are that it gives information about the proportion of pores with different diameters and it visualises well the pore structure [9–11].

The purpose of this paper is to evaluate the dependence of microporosity measured by high-pressure mercury porosimetry using pressure range of 0.1–227 MPa (pore diameter 8 μm–6.4 nm) and the dissolution rate of compressed erythromycin acistrate tablets. The main parameters describing porosity will also be discussed, i.e. total intruded volume, median of the intruded volume of mercury, pore diameter corresponding this median, pore size distribution and specific surface area of the pores.

Table 1
Characteristics of different erythromycin acistrate raw material batches ($n = 3$)

Raw material batch	Particle size (μm)			Specific surface area (m^2/g)
	50%	90%	10%	
1	17.1	56.5	5.5	2.3
2	17.7	41.8	5.5	1.7
3	17.5	44.2	5.9	1.8
4	20.2	50.7	5.4	1.7
5	24.6	77.2	6.5	2.1
6	13.7	44.1	3.5	1.8
7	14.4	34.2	4.5	2.0
8	14.4	34.2	4.5	2.0

Average error was estimated to be less than 10%.

2. Materials and methods

The active ingredient used in this study was erythromycin acistrate (stearate salt of acetylerythromycin, Orion Pharmaceutica, Espoo, Finland). Erythromycin acistrate is a prodrug of erythromycin in which an acetyl group is attached to the 2′-position of erythromycin by ester linkage [12]. The molecular structure of erythromycin acistrate is shown in Fig. 1.

The amount of erythromycin acistrate in the tablets was over 80%. Eight different tablet batches were used. Erythromycin acistrate was dry granulated. The tablets were compressed using a rotary tablet press (Fette P II, Fette, Germany). Magnesium stearate was used as a lubricant. The average weight of the capsule tablets (9 × 19 mm) was about 850 mg.

The microporosity of the tablets was determined by a high-pressure mercury porosimeter (Autoscan 33 Porosimeter, Quantachrome, USA) using a pressure range of 0.1–227 MPa which corresponds to a pore diameter of 8 μm–6.4 nm. The surface tension and the contact angle values used in calculations for mercury were 480 mN/m and 140°, respectively, as proposed earlier. Three tablets were placed into a capillary sample cell which was closed, evacuated and filled with mercury. Under increasing pressure the mercury penetrated into the pores and the level of mercury in the capillary decreased. A porosimetric curve was obtained when the decrease of the level was registered and presented as a function of pressure. The total intruded volume of mercury (V_{tot}) and the volume pore size distribution *Dv(d)* were calculated from the intrusion data. *Dv(d)* was calculated using Eq. (2)

$$Dv(d) = \frac{P}{d} \times \frac{dV}{dvP} \quad (2)$$

where P is pressure, d is pore diameter and V the intruded volume of mercury [4].

The true density of the tablets was determined using a helium pycnometer (Multipycnometer MPV-1, Quantachrome) method [13]. The measurements were made in triplicate by placing six tablets in a micro sample cell. The final densities were calculated using the following equation:

$$V_t = V_C - V_R(P_1/P_2 - 1) \quad (3)$$

where V_t is volume of the sample, V_C is volume of the sample cell, V_R is the known reference volume, P_1 is atmospheric pressure and P_2 pressure change during determination.

The specific surface area of raw materials and dry granulated mass was measured by BET-method (Flowsorb II 2300, Micromeritics Instrument, USA). Before determination the samples were dried in a vacuum oven (Heraeus VTR 5022, Leybold-Heraeus, Germany) for 20 h at a temperature of 40°C. The gas mixture contained 30.4/69.6% of nitrogen in helium. The measurements were made in triplicate.

Particle size distributions of erythromycin acistrate samples (raw material and dry granulated mass) were determined by a laser light diffraction method (Malvern 2600c Droplet And Particle Sizer, Malvern Instruments, UK). The focal length was 1000 mm and the particles were dispersed in air. Three parallel measurements were made. Fractiles of 10%, 50% and 90% are given in Tables 1 and 2.

The dissolution of erythromycin acistrate tablets was determined using USP XXII paddle method [14]. The dis-

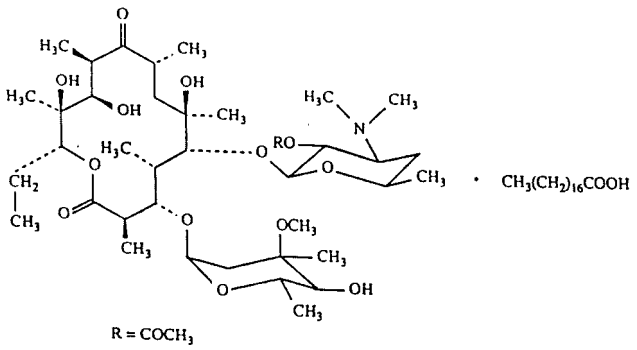

Fig. 1. Chemical structure of erythromycin acistrate raw material.

Table 2
Characteristics of the dry granulated mass batches

Dry granulated mass	Particle size (μm)[a]			Specific surface area (m^2/g)[b]	Bulk volume (ml)[c]	Tap volume (ml)[d]	Hausner ratio
	50%	90%	10%				
1	280	455	14	2.0	99.3	82.3	1.21
2	880	1470	60	1.6	102.7	82.0	1.25
3	850	1460	75	1.7	100.3	83.3	1.20
4	850	1470	55	1.8	103.3	84.3	1.23
5	790	1440	53	2.3	100.0	83.3	1.20
6	880	1490	60	1.5	94.0	80.0	1.18
7	800	1400	60	1.9	99.7	81.7	1.22
8	800	1400	90	1.7	101.7	84.0	1.21

Average error was estimated to be less than [a]24%, [b]10%, [c]1%, [d]0.6%.

solution medium was 900 ml of ethanol-phosphate buffer solution, pH 6.8. The rotation speed was 75 rpm. Six tablets were studied from every batch. The dissolution data was fitted using Eq. (4) originally published by Wiegand and Taylor [15].

$$D(t) = a(1 - e^{-bt}) + c \quad (4)$$

where $D(t)$ is the drug dissolved in time t, a is an amplitude of exponential, b is the rate constant, and c is zero intercept. The exponential starts at c ($b > 0$) and rises to $a + c$ with a time constant of $1/b$.

The surface structure of the raw material was studied using a scanning electron microscope (JEOL, JSM-840A Scanning Microscope, Japanese Electron Optics, Japan). The crushing strength (Erweka TBH28, Erweka Apparatebau, Germany) and disintegration time (Erweka ZT3–4, Erweka) of the tablets were determined using standard methods described in European Pharmacopoeia [16].

3. Results and discussion

3.1. Raw material

Surface morphology of erythromycin acistrate raw material is seen in Fig. 2a–c. The figures show that particle shape is quite irregular and also particle size seems to differ between batches. The particle size distribution and specific surface area are presented in Table 1. The particle size distribution between batches differs significantly, the mean particle size ranging from 13.7 to 24.6 μm. The specific surface area of the samples was about 2 m^2/g. Owing to a great variation between parallel tests in specific surface area determinations, differences between batches could not be verified.

3.2. Dry granulated mass

Particle size, specific surface area, bulk and tap volume and Hausner ratio (bulk volume/tap volume) of dry granulated mass are shown in Table 2. The only significant difference between the dry granulated mass batches was found in batch 1 where the mean particle size was 280 μm. In other batches the same parameter ranged from 790 to 880 μm. However, this particle size difference does not correlate with the other parameters presented in Table 2.

3.3. Tablets

Crushing strength, friability, disintegration time and true density of the tablets are given in Table 3. The crushing strength of batches E and F was the lowest and their friability, as expected, the highest. Average disintegration time in every batch was less than 90 s. Because of the great variation between parallel tests the disintegration times of different batches are not significantly different from each other. The true densities of the samples have approximately the same numerical value. This is expected because the helium molecule, being so small, can penetrate into very small holes in tablet structure and thus macrophysical processing such as dry granulation or compression cannot affect this parameter.

Dissolution results are presented in Fig. 3. The curves in the figure are calculated using Eq. (4). The experimental points in the figure are the average of six measurements. The values of curve fitting parameters are given in Table 4. Fig. 3 shows that the function used is able to approximate dissolution data quite acceptably.

A summary of the porosity of erythromycin acistrate tablets is given in Table 5. Figs. 4 and 5 show the total intruded volume of mercury and pore size distribution, respectively. Table 5 shows that intruded volume of mercury is highest in batches E and F. This is also seen in the median of the intruded volume of mercury and in the pore diameter at the median. The specific surface area of the pores has the highest value in batch A. This is perhaps caused by the small particle size of the batch (see Table 2). Also, Fig. 4 shows that the intruded volume of mercury is highest in batches E and F. This is very surprising because the dissolution rate of batch F is clearly the lowest. This

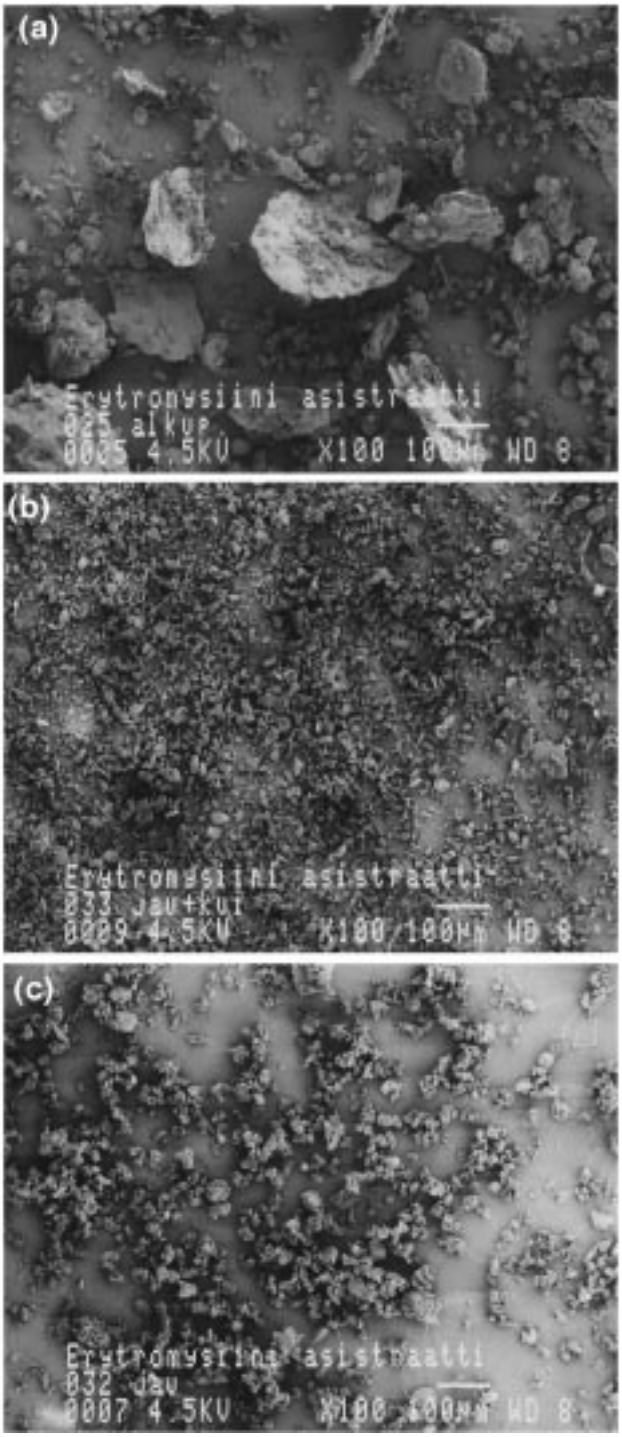

Fig. 2. (a–c) Typical SEM photographs of erythromycin acistrate raw material.

means that the dissolution of erythromycin acistrate tablets cannot be explained simply by intruded volume of mercury using the high pressure range that corresponds to pores less than 8 μm in diameter. It seems in the first place evident that no correlation between the number of small pores and dissolution rate may exist.

On the basis of Fig. 5a, peak values of the pore size distribution in batches B, C and D are quite near to each other and clearly greater than in batch A. This seems to explain the slower dissolution rate of batch A (Fig. 3b). In Fig. 5b, peak values of the pore size distribution of batches G and H are somewhat smaller than for batches B, C and D but greater than that of batch A (Fig. 5a). However, the dissolution rate of batches G and H seems to be slower than of batches A, B, C and D. Pore size distributions of batches E and F are exceptionally wide compared to the other batches. The number of pores in batch E is clearly greater than in batch F, which explains the more rapid dissolution of batch E.

In this case it is, however, difficult to make exact comparisons between all the batches studied because the pore size distributions have such a different structure.

Table 3

Some physical properties of erythromycin acistrate tablets

Tablet batch	Crushing strength (N) (n = 10)[a]	Friability (%) (n = 1)[b]	Disintegration time (s) (n = 6)[c]	True density (g/cm^3) (n = 6)[d]
A	130	0.22	90	1.17
B	153	0.20	88	1.16
C	124	0.19	49	1.16
D	130	0.11	40	1.16
E	98	0.39	60	1.19
F	90	0.28	40	1.16
G	136	0.18	46	1.16
H	140	0.16	90	1.17

Average error was estimated to be less than [a]12%, [b]6%, [c]40%, [d]0.5%.

3.4. The correlation matrix

The Pearson correlation matrix was calculated using the SAS statistical program package (SAS Institute, Cary, NC, USA) and a VAX/VMS operating system (Digital Equipment Corp., Maynard, MA, USA). The whole correlation matrix consisted of 37 different parameters. The most significant correlation coefficients and significance levels are given in Table 6. The symbols used are explained in the footnotes of the tables.

The porosity parameters of the tablets have no correlation with the dissolution results. However, the crushing strength

Table 4

The parameters of the fitted dissolution curves

Batch	a	b	c	R^2
A	62.31	0.836	25.25	0.998
B	68.12	0.862	29.35	0.999
C	65.10	1.227	26.48	0.998
D	80.38	1.319	16.14	0.999
E	71.20	1.748	23.43	0.998
F	42.11	0.838	27.06	1.0
G	55.43	1.051	23.05	0.998
H	59.63	1.263	23.34	0.992

a, amplitude of exponential; b, rate constant; c, zero intercept; R^2, coefficient of determination.

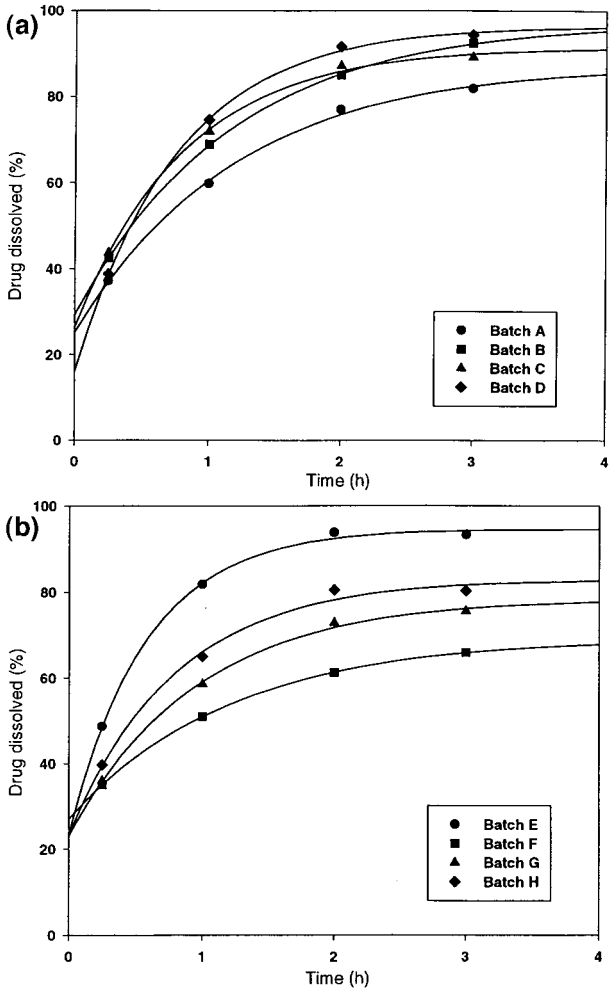

Fig. 3. (a) The dissolution curves of batches A, B, C and D. (b) The dissolution curves of batches E, F, G and H.

of the tablets has many significant negative correlations with porosity parameters (Table 6). When the crushing strength of the tablets increases, the total porosity and the amount of large pores (>1 μm) decreases ($P < 0.01$). The median of the intruded volume of mercury ($P < 0.01$) as well as the diameter of the pores corresponding this median ($P < 0.05$)

Table 5
The porosity of different erythromycin acistrate tablets

Tablet batch	Intruded volume of Hg (cm^3/g)[a]	Specific surface area of the pores (m^2/g)[b]	Median of the intruded Hg (cm^3/g)[c]	Pore diameter at the median (μm)[d]
A	0.133	13.1	0.067	0.139
B	0.135	12.2	0.068	0.189
C	0.150	12.1	0.075	0.226
D	0.157	11.9	0.077	0.233
E	0.196	12.9	0.098	0.244
F	0.209	12.4	0.106	0.413
G	0.147	13.0	0.074	0.158
H	0.164	12.9	0.082	0.183

Average error was estimated to be less than [a]5%, [b]2%, [c]6%, [d]8%.

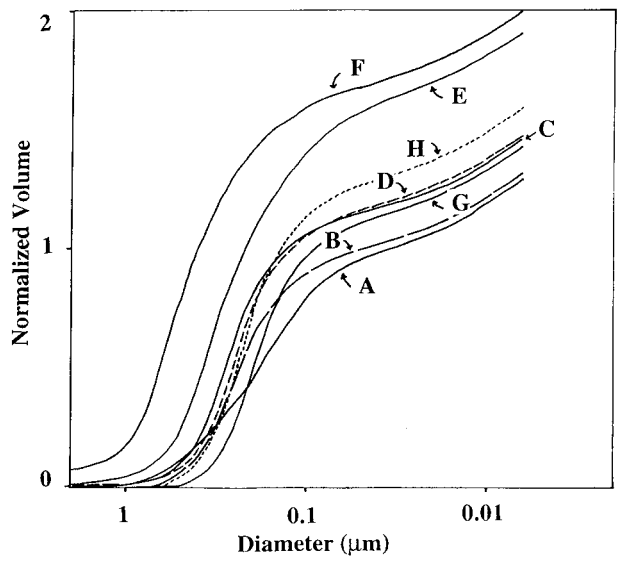

Fig. 4. The total pore volume (normalized volume of intruded mercury, $cm^3/g\ 10^{-2}$) of erythromycin acistrate tablets within the pressure range of 0.1–227 MPa.

decrease when the crushing strength of the tablets increases. It is obvious that with increasing compression force, the porosity of the tablets decreases and pore size distribution is shifted to smaller pore diameters.

Friability of the tablets has a negative correlation with crushing strength, as expected (Table 6). It is quite surprising that neither crushing strength nor friability of the tablets has a correlation with dissolution parameters (Table 6). However, bulk and tap volumes of the granulated mass have an interesting positive correlation with dissolution parameters (Table 6). When the bulk and tap volumes of the mass increase the dissolved amount of the drug increases, but the time when 50% of the tablets has dissolved decreases ($P < 0.05$). In any case the bulk or tap volumes of the tablet mass have no correlation with porosity parameters of the tablets.

In addition to the data shown in Table 6, it can be mentioned that according the correlation matrix the specific surface area of the raw material has a positive correlation with the surface area of the pores ($P < 0.01$). Also, the mean particle size of the raw material correlates positively with the dissolved amount of the drug in 120 min and 180 min ($P < 0.05$).

In general, it is very difficult to explain the dissolution of erythromycin acistrate tablets only by porosity, because the synthesis of the raw material and the processing parameters (compaction and tableting) affect porosity and also the dissolution rate of the tablets.

4. Conclusions

The pore size distribution of erythromycin acistrate tablets shows a difference in pore structure. It is evident

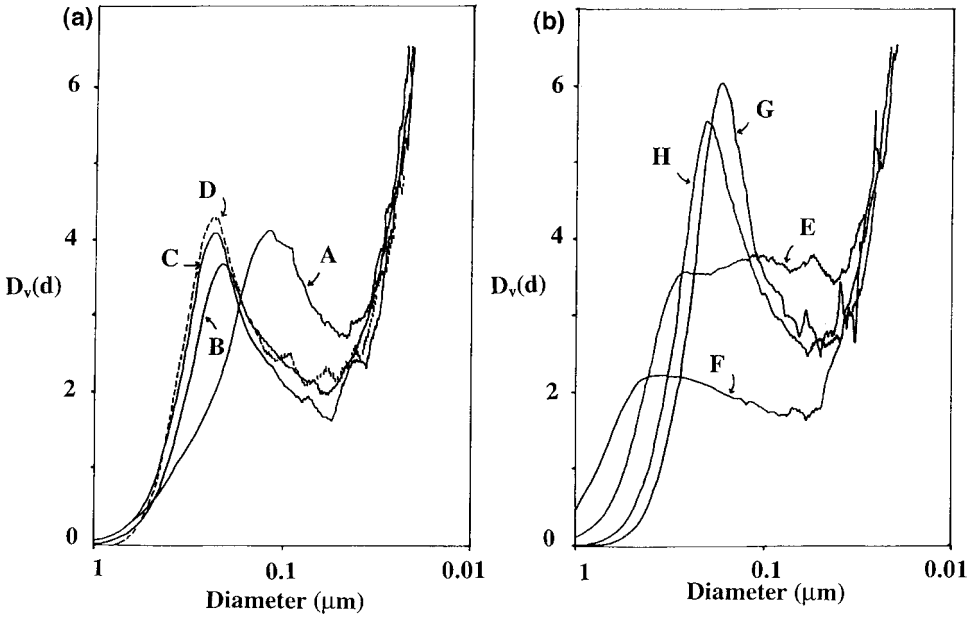

Fig. 5. (a) The pore size distribution *Dv(d)* ($cm^3/\mu m\ 10^{-1}$) of erythromycin acistrate batches of A, B, C and D within the pressure range of 0.1–227 MPa. (b) The pore size distribution *Dv(d)* ($cm^3/\mu m\ 10^{-1}$) of erythromycin acistrate batches of E, F, G and H within the pressure range of 0.1–227 MPa.

Table 6

The Pearson correlation matrix; correlation coefficients and significance levels ($n = 8$)

	A	B	C	D	E	F	G	H	I	J	K	L	M	N
Crushing strength (N)	–	–0.8830	–0.8823	–0.8003	–0.8851	–0.7781	–	–	–	–	–	–0.7208	–	–
	–	0.004	0.004	0.017	0.003	0.023	–	–	–	–	–	0.044	–	–
Friability (%)	0.7645	0.7194	0.7284	–	0.7241	–	–	–	–	–	0.8688	0.9306	–0.7941	–
	0.027	0.044	0.040	–	0.042	–	–	–	–	–	0.005	0.001	0.019	–
Bulk volume (ml)	–	–	–	–0.7718	–	–	–	0.7919	0.8147	–0.7272	–	–	0.7557	–
	–	–	–	0.025	–	–	–	0.019	0.014	0.041	–	–	0.030	–
Tap volume (ml)	–	–	–	–	–	–	0.7609	0.8355	0.7332	–0.7631	–	–	–	0.8012
							0.028	0.010	0.038	0.027	–	–	–	0.017

A, True density (g/cm^3); B, intruded volume of mercury (cm^3/g); C, intruded volume of mercury in pores >1 μm; D, d*V*/d*P* function; E, median of intruded volume of mercury (cm^3/g); F, diameter of pores corresponding the median of intruded volume of mercury (μm); G, dissolved amount of the drug (%) in 60 min; H, dissolved amount of the drug (%) in 120 min; I, dissolved amount of the drug (%) in 180 min; J, time for 50% of the drug has dissolved (min); K, particle size (μm), 90% fractile; L, specific surface area of the mass (m^2/g); M, crushing strength (N); N, bulk volume (ml).

that the pore size distribution can, to some extent, explain the dissolution rate of the tablets.

However, the dissolution behaviour of erythromycin acistrate tablets cannot be explained only by the volume of intruded mercury. The material used, erythromycin acistrate, is a stearate salt of acetylerythromycin and is therefore quite hydrophobic. The porosimetric method uses very high external pressure to force mercury into the pores and may thus ignore the nature of the surface; this rather illustrates the inner structure of the tablet, whereas during the dissolution process the penetration of the dissolution medium is more dependent on the surface properties of the tablet. These two methods illustrate the structure of the tablet in two different ways. Therefore the hydrophobicity of the material may have diverse effects on the results.

The surface structure and the mechanical properties of tablets warrant further studies.

References

[1] E.W. Washburn, The dynamics of capillary flow, Phys. Rev. 17 (1921) 273–283.
[2] J. van Brakel, S. Modry, M. Svata, Mercury porosimetry: state of the art, Powder Technol. 29 (1981) 1–2.
[3] Quantachrome Corporation, Autoscan 33 Porosimeter Guidebook, Quantachrome Corporation, Syosset, NY, USA, 1987.
[4] H.L. Ritter, L.C. Drake, Pore-size distribution in porous materials. Pressure porosimeter and determination of complete macropore-size distribution, Ind. Eng. Chem. 17 (1945) 782–786.
[5] W.A. Strickland, L.W. Busse, T. Higuchi, The physics of tablet compression: XI. Determination of porosity of tablet granulations, J. Am. Pharm. Assoc. 45 (1956) 482–486.
[6] P.J. Dees, J. Polderman, Mercury porosimetry in pharmaceutical technology, Powder Technol. 29 (1981) 187–197.
[7] F. Carli, P. Italiano, Effect of microstructure on liquid capillary penetration into porous drug carriers, in: S.J. Gregg, K.S.W. Sing, H.F. Stoeckli (Eds.), Characterisation of Porous Solids, Proc. Symp., Soc. Chem. Ind., London, 1979, pp. 369–374.

[8] A.B. Selkirk, D. Ganderton, An investigation of the pore structure of tablets of sucrose and lactose by mercury porosimetry, J. Pharm. Pharmacol. 22 (1970) 79S–85S.
[9] A.M. Juppo, J. Yliruusi, Effect of amount of granulation liquid on total pore volume and pore size distribution of lactose, glucose and mannitol granules, Eur. J. Pharm. Biopharm. 40 (1994) 299–309.
[10] A.M. Juppo, Change in porosity parameters of lactose, glucose and mannitol granules caused by low compression force, Int. J. Pharm. 130 (1996) 149–157.
[11] A.M. Juppo, Porosity parameters of lactose, glucose and mannitol tablets obtained by mercury porosimetry, Int. J. Pharm. 129 (1996) 1–12.
[12] U.S. Patent no. 4,599,326 issued to Orion Corp. (7.8.1986).
[13] Quantachrome Corporation, Helium Pycnometer Guidebook, Quantachrome Corporation, Syosset, NY, USA, 1987.
[14] The United Stated Pharmacopeia XXII, The United Pharmacopeia Convention, Rockville, MD, 1989.
[15] R.G. Wiegand, J.D. Taylor, Kinetics of plasma drug levels after sustained release dosage, Biochem. Pharmacol. 3 (1960) 256–263.
[16] European Pharmacopoeia, Second Edition, Maisonneuve, France, 1980.